



Original Paper

Reclassification and distribution patterns of discovered oils in the Dongying Depression, Bohai Bay Basin, China

Bing You ^{a, b}, Jian-Fa Chen ^{a, b, *}, Zhi-Yong Ni ^{a, b, **}^a State Key Laboratory of Petroleum Resource and Prospecting, China University of Petroleum, Beijing, 102249, China^b School of Geoscience, China University of Petroleum, Beijing, 102249, China

ARTICLE INFO

Article history:

Received 25 February 2022

Received in revised form

6 May 2022

Accepted 11 August 2022

Available online 28 August 2022

Edited by Jie Hao

Keywords:

Molecular biomarker

Oil-oil correlation

Oil distribution

Kongdian Formation

Dongying Depression

ABSTRACT

The Dongying Depression is an important petroliferous province, with diverse source rocks and complex petroleum distribution patterns. A total of 32 crude oils were analyzed by the gas chromatography–mass spectrometry and isotopic compositions to better understanding the petroleum systems in the study area. Three oil types were classified by hierarchical cluster analyses. Type I and II oils have closely correlation with the discovered source rocks, which have been confirmed to be mainly derived from the lower third and upper fourth member of the Eocene Shahejie Formation source rocks (Es3^L and Es4^U), respectively. Obviously, type III oils contain abundant gammacerane, tricyclic terpanes and C₂₉ steranes and have lower values of δ¹³C than type I and II oils, indicating a completely different source rock and biological origins. Until recently, type III oils fail to match any of the discovered source rock, which contains main contribution of aquatic organism or/and bacteria inputs. In addition, the spacial distribution of these three oil types were discussed. Type I oils mainly distributed in the Es3 and Es4 reservoirs that closed to the generative kitchens. Type II oils occurred in the Es4 reservoirs in the southern slope of the depression, which probably caused by lateral migration along the horizontal fractures and sandstone layers within the Es4 interval. Differently, type III oils in the southern slope of the depression were mainly discovered in the Eocene Kongdian or Ordovician reservoirs, which suggests great exploration potential of deep underlying strata.

© 2023 The Authors. Publishing services by Elsevier B.V. on behalf of KeAi Communications Co. Ltd. This is an open access article under the CC BY-NC-ND license (<http://creativecommons.org/licenses/by-nc-nd/4.0/>).

1. Introduction

As a significant petroliferous area of the Bohai Bay Basin, the Dongying Depression developed the fourth member and (Es4) and the third member (Es3) of the Eocene Shahejie Formation as two sets of effective source rocks (Li et al., 2003; Zhu et al., 2004a; Zhang et al., 2009). The organic petrological and geochemical analyses studies of these source rocks have been studied well (Zhang et al., 2003, 2009; Liu et al., 2009; Li et al., 2010). Moreover, the Es3^L source rock was confirmed to deposit in a freshwater to brackish lacustrine environment and the organic matter is composed of aquatic organisms and a small quantity of higher plants. While the

Es4^U source rock was formed in a brackish and saline water lacustrine environment with the predominant organic matter inputs of aquatic organisms (Li et al., 2003; Zhu and Jin, 2003; Pang et al., 2003; Zhang et al., 2009). The Es3^L source rock has some typical geochemical features of moderate Pr/Ph values, low value of gammacerane index, high content of C₂₇ diasterane and 4-methylsteranes, whereas the Es4^U source rock contains the biomarkers of extremely low Pr/Ph ratio, high value of gammacerane index, an obvious “rise” of C₃₅ homohopane, and low abundances of C₂₇ diasterane and 4-methylsteranes (Pang et al., 2003; Li et al., 2003, 2005, 2010; Zhang et al., 2003, 2009; Zhu and Jin, 2003; Zhu et al., 2004a). Generally, the discovered oil reservoirs in the study area are considered to be mainly originated from the source rocks of Es3^L and Es4^U (Zhang et al., 2003, 2009; Zhu et al., 2004a), which control the formation of the large oil fields with hundred million tons of oil production (Zhu and Jin, 2003). Recently, a distinct oil type with markedly different molecular marker compositions has been discovered in the southern areas of the depression and furtherly investigated. This new type of crude oil

* Corresponding author. State Key Laboratory of Petroleum Resource and Prospecting, China University of Petroleum, Beijing, 102249, China.

** Corresponding author. State Key Laboratory of Petroleum Resource and Prospecting, China University of Petroleum, Beijing, 102249, China.

E-mail addresses: jfchen@cup.edu.cn (J.-F. Chen), nizhy@cup.edu.cn (Z.-Y. Ni).

was proposed to have mixed sources, likely from the potential source rocks of the Es4 member of the Shahejie Formation and the Ek2 member of the Kongdian Formation (Li et al., 2005), or from the Es4^U and another source rock that deposited in shallow water sedimentary facies (Meng et al., 2011). But some hold that these oils have unmixed sources based on the chemometric analysis (Zhan et al., 2019) and molecular marker compositions (e.g. norcholestane and triaromatic steroid) (You et al., 2021). Niu et al. (2021) also identified this type of oil by the trace element analysis of crude oils in the southern slope. In addition, Wang et al. (2021) found that the biomarkers including steranes, terpanes, β -carotane and aromatic steroids of the Mesozoic sediments are mostly absent due to the high thermal maturity of the rock extracts. Because of the lack of the exploration and understanding of the Kongdian Formation and its underlying strata, the related source rocks of these oils remain unsolved.

Moreover, the spatial distribution of crude oils in the Dongying Depression is also complex, including horizontal and vertical distributions. The previous studies about the oil distribution patterns mainly focused on the Es3^L-derived oil and/or the Es4^U-derived oil, but lacked understanding of the distinct oil type. Zhang et al. (2003) found that the Es3^L-derived oils are mainly distributed in the north and center of depression, whereas the Es4^U-derived oil are mainly charged into the south slope and the edge of depression. Li (2004) proposed a ring pattern of crude oil distribution and from the inner ring to the outer ring oil changes from light to heavy in the Dongying Depression.

In this study, the crude oils were investigated by bulk properties, biomarker compositions and stable carbon isotope, and discriminated based on the geochemical analysis and the hierarchical cluster analysis. Moreover, the spatial distribution of three oil types were further analyzed. This work is designed to better understand the origin and distribution of oil samples and will provide new insights for further petroleum exploration in the Dongying Depression.

2. Geological setting

The Dongying Depression is a sub-structural unit of the Jiyang sub-basin in the southeastern Bohai Bay Basin, with a total area of 5850 km² (Zhang et al., 2009). It has experienced two main stages of tectonic evolution, namely the syn-rift and the post-rift stages (Huang and Pearson, 1999). During the syn-rift stage, the Paleogene Kongdian (Ek), Shahejie (Es) and Dongying formations (Ed) formed, and the Neogene Guantao (Ng), Minghuazhen (Nm) and Quaternary Pingyuan formations (Qp) were developed in the post-rift stage (Fig. 1c). The Kongdian Formation was formed overlying the Mesozoic metamorphic basement, and mainly comprised of coarse clastic red-beds (Li et al., 2003). The Shahejie Formation contains the most important petroleum system in the Dongying Depression and was mainly developed in the fluvial and lacustrine facies (Pang et al., 2003; Zhu et al., 2004a), which can be further subdivided into four members, including member IV (Es4), member III (Es3) member II (Es2) and member I (Es1) from bottom to top (Fig. 1c). And the mudstones were well developed in the Es4^U and Es3^L as the most effective source rocks (Zhu et al., 2004a; Zhang et al., 2009). The considerable contribution from these two source rocks has been found in several oilfields, such as the Shengtuo, Liangjialou, Bamianhe oilfields, and so on (Zhu et al., 2004b; You et al., 2020; Zhan et al., 2019).

The northern basement-fault made the Dongying Depression a typical asymmetric “dustpan shaped” lacustrine basin. Five secondary tectonic units from the north to south are the Northern Steep Slope Zone, Northern Sag Zone, Central Anticline Zone, Southern Sag Zone and Southern Gentle Slope Zone. The Northern

Sag Zone contains the Minfeng and Lijin sags, whereas the Niuzhuang and Boxing sags are in the southern sag zone (Zhu et al., 2004a; Ping et al., 2017) (Fig. 1b). In the Northern Steep Slope Zone, a nearshore subaqueous fan (Minfeng and Shengtuo areas) and fan delta (Lijin area) were developed during the syn-rift stage, hence plentiful terrigenous clastic materials were injected into the center of the Northern Sag Zone. However, the formation thicknesses in the southern of the depression were much thinner.

3. Samples and methods

3.1. Samples

A total of 32 crude oils were collected for oil-oil correlations analysis, fifteen from the Es3 member, twelve from the Es4 member, two from the Kongdian Formation and three from the Ordovician carbonate reservoirs. These selected oil samples are widely covered in several oilfields, such as the Zhenjia (ZJ), Shengtuo (ST), Xianhe (XH), Liangjialou (LJL), Niuzhuang (NZ), Wangjiagang (WJG) and Bamianhe (BMH) oilfields. Well locations of these crude oils are shown in Fig. 1b.

3.2. GC–MS analysis

Saturated hydrocarbon, aromatic hydrocarbon, and resin fractions of all the crude oils were acquired by a standard column liquid chromatography. The gas chromatography–mass spectrometry (GC–MS) analysis of saturated hydrocarbon fraction in all the crude oils was performed for further investigate the molecular marker compositions. An Agilent 6890 GC instrument with an Agilent Model 5975i Mass Selective Detector was applied for GC–MS analysis. HP-5 MS fused silica capillary column (30 m × 0.25 mm inter diameter, 0.25 μ m thick) was used. The carrier gas was He at constant flow (1 mL/min). The initial GC oven temperature was at 50 °C, (held 1 min), and increased to 100 °C at a rate of 20 °C/min, then ramped to 310 °C at 3 °C/min (held 10 min).

3.3. Stable carbon isotope analysis

Crude oils and their four fractions were analyzed by the MAT 253 isotope ratio mass spectrometer to measure their stable carbon isotope, conducting standard sealed tube combustion methods. The FLASH HT EA reactor was full of chromium oxide, copper, and cobalt oxide that containing silver, and carbon was changed into carbon dioxide at 980 °C in it. The δ notation was used to state the carbon isotope values in parts per thousand (‰), which compared with the International Atomic Energy Agency-600 caffeine standard.

4. Results and discussion

4.1. Bulk properties of crude oils

The physical property results show densities ranging from 0.81 to 0.90 g/cm³ for most of oil samples, while five oils have densities higher than 0.90 g/cm³, and four oil samples with no relevant data (Table 1). It can be seen that these crude oils are dominantly the light to medium oils, and some oils with densities greater than 0.90 g/cm³ were considered to be affected by biodegradation. Viscosity of the crude oils is mainly in the range of 1.24–56.00 mPa s, and a few oils with extremely high viscosity ranging from 100.00 to 16287.00 mPa s are biodegraded oils (Table 1). Most crude oils contain low sulfur content (<1.0%), but biodegraded oils show relatively higher sulfur content. In addition, all the oils are dominated by saturated hydrocarbons (Table 1), but biodegraded oils have lower saturated hydrocarbon amounts and higher

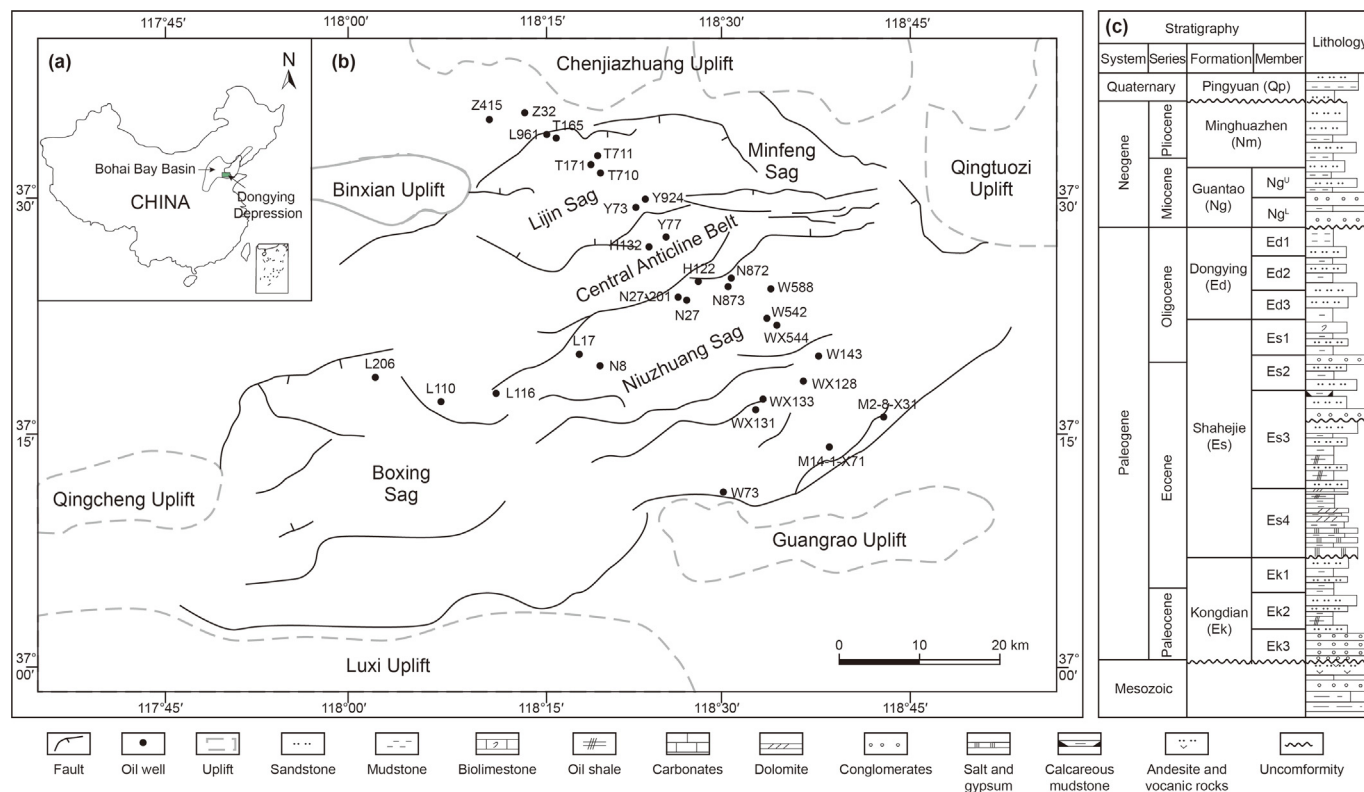


Fig. 1. (a) Location of the Dongying Depression, (b) locations of sampling wells and (c) stratigraphy of the Dongying Depression.

Table 1 Bulk properties and fraction compositions of crude oils in the Dongying Depression.

Sm. No.	Well	Depth, m	Strata	Oilfields	Density, g/cm ³	Viscosity, mPa s	Sulfur content, %	Saturate, %	Aromatic, %	Resin, %	Asphaltene, %
1	W542	3147.4–3162.2	Es3	WJG	0.85	8.13	0.12	67.81	15.75	10.27	6.16
2	WX544	2826.0–2829.4	Es3	WJG	0.87	20.20	0.27	56.42	18.24	14.53	10.81
3	L17	2903.2–2921.4	Es3	LJL	/	/	/	66.05	15.53	16.84	1.58
4	N872	3040.8–3049.2	Es3	NZ	0.87	23.50	0.24	62.63	13.98	18.55	4.84
5	N27	3271.2–3277.0	Es3	NZ	0.90	17.90	0.38	59.24	10.60	18.21	11.96
6	N873	3243.9–3255.4	Es3	NZ	0.90	16.70	0.31	58.18	16.98	7.86	16.98
7	H122	3023.4–3026.8	Es3	XH	0.87	14.60	0.30	61.31	15.08	12.79	10.82
8	H132	2826.0–2828.0	Es3	XH	0.90	56.00	0.49	46.95	18.33	15.76	18.97
9	Y73	2850.0–2894.0	Es3	XH	0.87	22.90	0.40	53.44	15.63	14.37	16.56
10	Y77	3096.7–3107.6	Es3	XH	0.87	19.50	0.36	55.09	17.19	12.98	14.74
11	Y924	2711.0–2714.0	Es3	XH	0.87	19.90	0.23	56.46	15.65	13.61	14.29
12	L961	2419.6–2425.0	Es3	ST	0.86	14.20	0.19	54.51	17.65	16.08	11.76
13	T165	2551.9–2555.4	Es3	ST	0.85	8.86	0.21	60.78	17.32	13.73	8.17
14	T711	3119.6–3209.9	Es3	ST	0.85	7.36	0.08	64.42	21.17	11.96	2.45
15	T165	3385.1–3397.1	Es4	ST	0.81	1.24	0.07	75.67	12.76	6.82	4.75
16	T710	3792.9–3802.3	Es4	ST	0.84	3.73	0.11	72.89	17.61	7.75	1.76
17	T171	3295.4–3349.4	Es4	ST	0.88	19.70	0.19	56.60	20.49	12.50	10.42
18	L110	2996.8–3032.0	Es4	LJL	0.87	14.20	0.13	62.15	18.77	10.77	8.31
19	L116	2931.0–2981.0	Es4	LJL	0.89	15.80	0.27	54.82	12.18	15.23	17.77
20	L206	2803.6–2818.0	Es4	LJL	0.86	11.80	0.14	61.49	16.42	10.45	11.64
21	N8	3081.4–3089.4	Es4	NZ	0.88	41.70	0.29	57.77	15.78	19.72	6.73
22	W588	3417.2–3427.6	Es4	WJG	0.86	9.72	0.20	60.00	18.52	15.19	6.30
23	Z32	1327.2–1333.2	Es3	ZJ	0.99	16287.00	0.78	22.36	21.41	28.12	28.12
24	Z415	1645.8–1650.0	O	ZJ	0.99	10330.00	0.66	31.87	24.37	24.69	19.06
25	N27-201	1285.6–1298.5	O	NZ	/	/	/	34.48	26.65	21.63	17.24
26	WX128	2616.7–2620.2	Es4	WJG	0.92	327.00	0.81	37.09	12.73	23.64	26.55
27	W143	2795.4–2801.0	Es4	WJG	0.94	100.00	0.64	57.19	16.29	13.10	13.42
28	W73	1285.0–1296.0	Es4	WJG	0.94	840.00	2.79	35.40	21.78	29.46	13.37
29	M2-8-X31	1541.6–1554.6	Es4	BMH	/	/	/	33.88	24.10	21.82	20.20
30	M14-1-X71	1544.0–1611.0	O	BMH	/	/	/	70.09	12.54	5.70	11.68
31	WX131	2467.3–2495.8	Ek	WJG	0.83	14.60	0.18	71.72	12.60	12.34	3.34
32	WX133	3179.4–3185.8	Ek	WJG	0.83	5.09	0.10	72.85	13.58	5.30	8.28

Note: Sm. No. = Sample number; '/' means no data.

nonhydrocarbon contents than normal oils. Samples No. 23–29 were considered to have suffered biodegradation, these oils mainly collected from the ZJ, WJG and NZ oilfields. Hence, biodegradation probably gave rise to the higher viscosity, density and sulfur content of the selected oils in this study. In short, except for several biodegraded oils, most oil samples are light to medium oils, containing low density, low viscosity and low sulfur content and dominant saturated hydrocarbons.

4.2. Thermal maturity

Several maturity parameters of crude oil were calculated and compared. Generally, maturity parameters have different applications because of their diverse reaction endpoints and responses. The C_{32} 22S/(22S + 22R) homohopane ratio of crude oils in this study ranges from 0.50 to 0.63, mostly in the range of 0.57–0.62 (Table 2, Fig. 2a), indicating that the related source rocks have reached the early oil generation phase (Peters et al., 2005). The C_{29} steranes 20S/(20S + 20R) and $\beta\beta/(\beta\beta + \alpha\alpha)$ ratios of crude oils were within the ranges of 0.24–0.48 and 0.26–0.55 (Table 2, Fig. 2b), illustrating a wide stage from immature to the peak oil generation (Peters et al., 2005). Although the Ts/Tm ratio was proposed to be occasionally affected by biogenic source and/or depositional conditions (Peters et al., 2005; Xiao et al., 2019c, 2021a), the values of Ts/Tm show positive linear relationships with C_{29} sterane 20S/(20S + 20R) (Table 2, Fig. 2c) (Zhan et al., 2019), which indicates that Ts/Tm ratio can effectively characterize thermal maturity in the study area.

Different oils show diverse maturity levels. The samples No. 26–29 have obviously lower maturity than the samples No. 1–25 and 30–32, which as the typical immature oils in the Dongying Depression were always considered to be derived from the Es4 source rock containing the sulfur-rich kerogen (Pang et al., 2003; Li et al., 2005), while the samples No. 1–25 and 30–32 have similar range of maturity and considered to be mature oils (Zhan et al., 2019). All oil samples have not yet reached high-over maturity level, thus thermal maturity is not a key factor for altering the biomarker compositions in the study area. Consequently, source- and depositional condition-related parameters can provide a reliable correlation between oils and their source in the study (Peters et al., 2005; Xiao et al., 2021b).

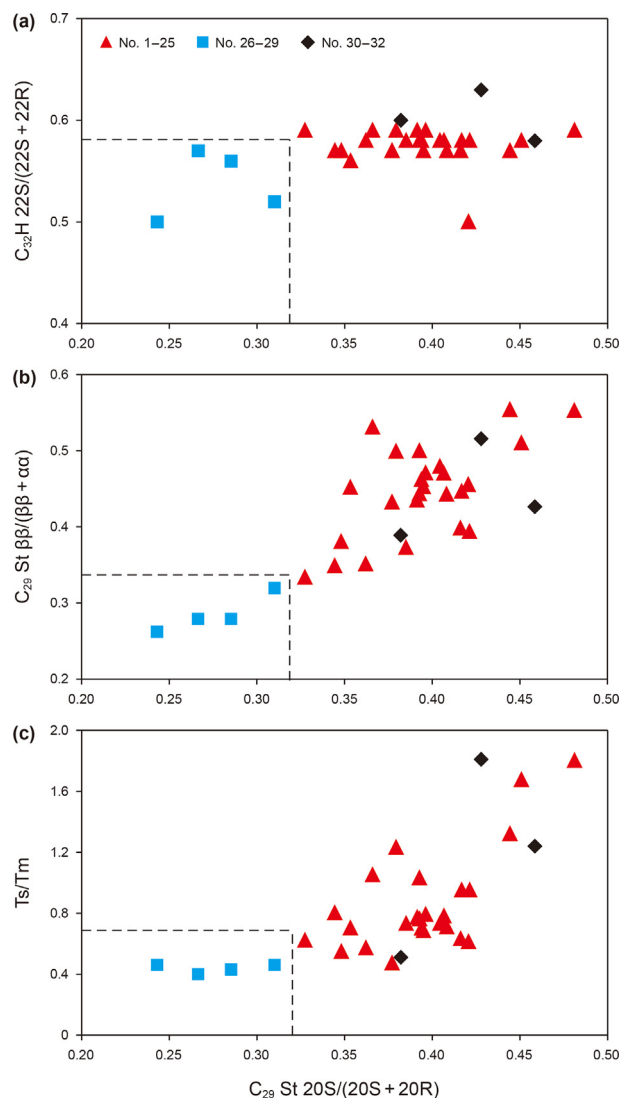


Fig. 2. Cross plots of C_{29} St 20S/(20S + 20R) vs. C_{30} H 22S/(22S + 22R) (a), C_{29} St 20S/(20S + 20R) vs. C_{29} St $\beta\beta/(\beta\beta + \alpha\alpha)$ (b) and C_{29} St 20S/(20S + 20R) vs. Ts/Tm (c) showing the different maturities of three oil types.

Table 2 Selected maturity-related parameters of crude oils in the Dongying Depression.

Sm. No.	Well	C_{29} St 20S/(20S + 20R)	C_{29} St $\beta\beta/(\beta\beta + \alpha\alpha)$	Ts/Tm	C_{32} H 22S/(22S + 22R)	Sm. No.	Well	C_{29} St 20S/(20S + 20R)	C_{29} St $\beta\beta/(\beta\beta + \alpha\alpha)$	Ts/Tm	C_{32} H 22S/(22S + 22R)
1	W542	0.37	Ts/Tm	1.05	0.59	17	T171	0.39	0.44	1.03	0.58
2	WX544	0.35	0.38	0.55	0.57	18	L110	0.40	0.47	0.79	0.59
3	L17	0.41	0.44	0.71	0.57	19	L116	0.41	0.47	0.78	0.58
4	N872	0.35	0.45	0.70	0.56	20	L206	0.39	0.43	0.77	0.59
5	N27	0.39	0.45	0.68	0.57	21	N8	0.42	0.40	0.63	0.57
6	N873	0.45	0.51	1.67	0.58	22	W588	0.38	0.43	0.47	0.57
7	H122	0.40	0.48	0.73	0.58	23	Z32	0.42	0.46	0.61	0.50
8	H132	0.39	0.50	0.76	0.58	24	Z415	0.36	0.35	0.57	0.58
9	Y73	0.42	0.45	0.95	0.58	25	N27-201	0.33	0.33	0.62	0.59
10	Y77	0.39	0.46	0.70	0.58	26	WX128	0.24	0.26	0.46	0.50
11	Y924	0.42	0.39	0.95	0.58	27	W143	0.31	0.32	0.46	0.52
12	L961	0.39	0.37	0.73	0.58	28	W73	0.27	0.28	0.40	0.57
13	T165	0.34	0.35	0.80	0.57	29	M2-8-X31	0.29	0.28	0.43	0.56
14	T711	0.38	0.50	1.23	0.59	30	M14-1-X71	0.38	0.39	0.51	0.60
15	T165	0.44	0.55	1.32	0.57	31	WX131	0.46	0.43	1.24	0.58
16	T710	0.48	0.55	1.80	0.59	32	WX133	0.43	0.52	1.81	0.63

Note: Sm. No. = Sample number.

4.3. Normal alkane and isoprenoid

Total ion current diagrams of saturated hydrocarbons show that most crude oils contain complete distribution of *n*-alkane series (nC_{13} – nC_{38}) except biodegraded oils, and maintain the predominance of phytane over pristane (Fig. 3a and b). The relative abundances of *n*-alkane series of most oils are higher than those of

acyclic isoprenoids (e.g. pristane and phytane, Pr and Ph). The samples No. 26–29 show abundance advantages of the acyclic isoprenoids over *n*-alkane series, and have the highest Ph/ nC_{18} (2.43–10.95) and Pr/ nC_{17} ratios (0.97–2.70) (Fig. 3c; Table 3), which probably due to the slight biodegradation that *n*-alkanes were partially consumed (Pang et al., 2003). Interestingly, the Es4 source rocks with depths of ~2700 m also exhibit the same characteristics

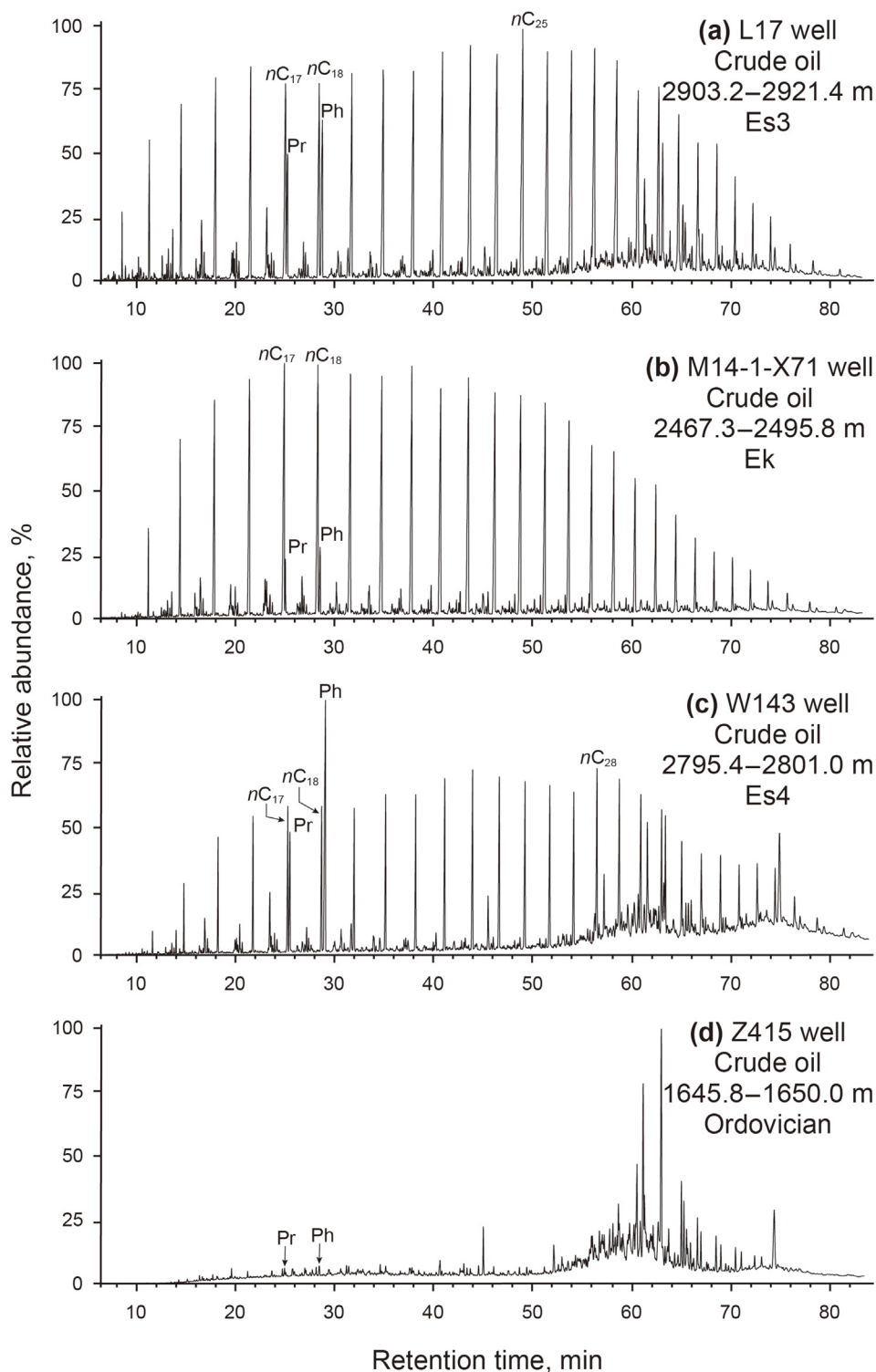


Fig. 3. The total ion current diagrams of the saturated hydrocarbons of oils in the Dongying Depression.

Table 3
Molecular parameters related to normal alkanes and acyclic isoprenoids of crude oils in the Dongying Depression.

Sm. No.	Well	Max. Peak	CPI	OEP	Ph/C ₁₈	Pr/C ₁₇	$n_{C_{21}}/n_{C_{22}+}$	$(C_{21}+C_{22})/(C_{28}+C_{29})$
1	W542	C23	1.03	0.99	1.11	0.59	0.65	1.22
2	WX544	C25	1.02	0.97	1.41	0.73	0.54	0.99
3	L17	C25	1.05	1.03	0.77	0.50	0.47	0.86
4	N872	C29	1.09	1.10	1.37	0.60	0.36	0.71
5	N27	C25	1.06	1.08	1.44	0.62	0.42	0.86
6	N873	C17	1.09	1.07	0.33	0.35	0.87	1.55
7	H122	C23	1.04	1.03	1.38	0.61	0.57	1.06
8	H132	C23	1.05	1.01	1.04	0.53	0.63	1.13
9	Y73	C25	1.06	0.99	0.86	0.48	0.56	1.05
10	Y77	C25	1.09	1.03	1.05	0.63	0.57	1.00
11	Y924	C25	1.10	1.08	0.71	0.50	0.65	1.15
12	L961	C23	1.12	1.10	1.10	0.62	0.64	1.27
13	T165	C23	1.13	1.07	0.87	0.53	0.78	1.39
14	T711	C23	1.00	0.96	1.35	0.65	0.66	1.09
15	T165	C16	1.00	0.94	1.58	0.76	1.58	2.19
16	T710	C17	1.09	1.07	0.26	0.32	0.98	1.44
17	T171	C23	1.11	1.02	0.49	0.48	0.68	1.29
18	L110	C25	1.05	0.98	0.87	0.62	0.54	0.96
19	L116	C25	1.00	0.95	1.51	0.70	0.49	0.90
20	L206	C25	1.05	1.00	0.74	0.50	0.61	1.14
21	N8	C28	1.05	0.98	1.05	0.59	0.41	0.74
22	W588	C25	1.11	1.06	1.21	0.55	0.70	1.24
23	Z32	/	/	/	/	/	/	/
24	Z415	/	/	/	/	/	/	/
25	N27-201	/	/	/	/	/	/	/
26	WX128	C28	1.10	0.95	5.90	1.50	0.37	0.67
27	W143	C28	0.94	0.86	2.43	0.97	0.41	0.88
28	W73	C18	0.93	0.84	6.13	1.46	0.79	1.61
29	M2-8-X31	C16	0.96	0.88	10.95	2.70	0.69	1.09
30	M14-1-X71	C13	1.02	1.02	0.32	0.16	0.82	1.20
31	WX131	C23	1.04	1.03	0.46	0.25	0.77	1.33
32	WX133	C23	1.06	1.06	0.19	0.13	0.79	1.57

Note: Sm. No. = Sample number; '/' means no data.

Table 4
Selected molecular parameters related to acyclic isoprenoids, tricyclic terpanes, tetracyclic terpane, hopanes and steranes of crude oils in the Dongying Depression.

Sm. No.	Well	R1	R2	R3	R4	R5	R6	R7	R8	R9	R10	R11
1	W542	0.54	0.20	0.65	0.18	0.58	1.60	0.045	0.47	0.35	0.46	0.48
2	WX544	0.54	0.18	0.70	0.16	0.63	1.40	0.028	0.74	0.31	0.48	0.54
3	L17	0.70	0.10	0.52	0.19	0.85	1.13	0.026	0.72	0.31	0.49	0.28
4	N872	0.45	0.17	0.50	0.16	0.62	1.61	0.033	0.60	0.25	0.46	0.39
5	N27	0.44	0.16	0.62	0.21	0.44	1.42	0.025	0.59	0.31	0.41	0.41
6	N873	1.08	0.05	0.49	0.16	0.97	0.76	0.026	0.58	0.49	0.73	0.24
7	H122	0.44	0.24	0.67	0.23	0.58	1.76	0.035	0.59	0.27	0.36	0.64
8	H132	0.51	0.16	0.78	0.30	0.79	1.18	0.024	0.64	0.33	0.40	0.36
9	Y73	0.58	0.13	0.64	0.34	0.67	1.26	0.031	0.70	0.29	0.41	0.34
10	Y77	0.65	0.10	0.65	0.52	0.80	1.09	0.024	0.68	0.32	0.49	0.37
11	Y924	0.77	0.08	0.59	0.18	0.82	1.10	0.024	0.71	0.30	0.51	0.30
12	L961	0.61	0.12	0.55	0.65	0.67	1.39	0.024	0.64	0.39	0.38	0.36
13	T165	0.68	0.11	0.77	0.46	0.82	1.04	0.020	0.62	0.34	0.34	0.24
14	T711	0.48	0.44	0.75	0.19	0.48	2.05	0.058	0.44	0.46	0.42	0.91
15	T165	0.52	0.42	0.86	0.88	0.54	2.11	0.094	0.42	0.41	0.40	0.41
16	T710	1.19	0.07	0.57	0.56	1.13	0.66	0.036	0.42	0.67	0.73	0.31
17	T171	1.43	0.06	0.52	0.57	1.00	0.85	0.019	0.65	0.53	0.97	0.20
18	L110	0.77	0.14	0.67	0.15	0.67	1.48	0.040	0.49	0.34	0.48	0.39
19	L116	0.44	0.27	0.63	0.16	0.57	1.74	0.040	0.60	0.27	0.34	0.67
20	L206	0.74	0.12	0.56	0.17	0.79	1.18	0.038	0.53	0.23	0.52	0.36
21	N8	0.60	0.14	0.53	0.13	0.67	1.38	0.027	0.63	0.26	0.52	0.29
22	W588	0.47	0.12	0.59	0.22	0.68	1.30	0.025	0.80	0.21	0.23	0.36
23	Z32	0.54	0.34	0.71	0.26	0.58	1.53	0.063	0.28	1.02	0.43	0.22
24	Z415	0.69	0.20	0.61	0.36	0.63	1.56	0.035	0.56	0.63	0.24	0.34
25	N27-201	0.46	0.17	0.91	0.26	1.02	0.86	0.035	1.04	0.30	0.32	0.27
26	WX128	0.34	0.51	1.15	0.15	0.67	1.69	0.041	0.73	0.11	0.06	2.55
27	W143	0.38	0.48	1.15	0.10	0.58	1.60	0.053	0.81	0.18	0.17	1.53
28	W73	0.25	1.35	1.17	0.15	0.50	1.97	0.038	0.96	0.11	0.15	3.61
29	M2-8-X31	0.32	0.97	1.30	0.19	0.49	2.29	0.046	1.03	0.14	0.14	3.33
30	M14-1-X71	0.53	1.09	0.80	0.14	0.25	3.14	0.236	0.38	0.32	0.17	1.10
31	WX131	0.58	1.37	0.65	0.13	0.36	3.09	0.245	0.27	0.33	0.16	0.63
32	WX133	0.66	1.91	0.89	0.13	0.34	3.15	0.288	0.26	0.42	0.17	0.40

Notes: Sm. No. = Sample number; R1=Pr/Ph; R2=G/C₃₀H; R3=C₃₅/C₃₄ 22S H; R4=C₁₉/C₂₃TT; R5=C₂₄TeT/C₂₆TT; R6=C₂₅TT/C₂₄TeT; R7=C₂₃TT/(C₂₃TT+C₃₀H); R8=C₂₇/C₂₉ aaAR St; R9 = C₂₇Dia/C₂₇St; R10 = 4-Me/C₂₉St; R11 = C₂₉St/C₃₀H.

with these oils (Zhang et al., 2003; Li et al., 2010), which means these oils probably inherit the characteristics of source rocks rather than slight biodegradation. Moreover, Pr/Ph ratio of these four oils are extremely low in the range of 0.25–0.38 (Table 4), which correlates well with the Es4^U source rocks (Pr/Ph ratio, <0.6) that deposited in a strongly anoxic and reductive depositional condition (Li et al., 2003; Zhu et al., 2004a). The Pr/Ph values of samples No. 1–25 and 30–32 are in the range of 0.44–1.43 with an average of 0.67 (Table 4), suggesting a slightly anoxic depositional condition of the related source rocks. Among these oils, three oils with buried depths less than 2000 m (Sm. No. 23–25) are confirmed to have suffered biodegradation. Not only their *n*-alkane series and acyclic isoprenoids are completely consumed (Fig. 3d), but also 25–norhopane homologous series have been identified (Volkman et al., 1983; Bennett et al., 2006).

The values of $\sum C_{21}-\sum C_{22+}$, $(C_{21}+C_{22})/(C_{28}+C_{29})$, carbon preference index (CPI), and odd-even predominance (OEP) of crude oils were listed in Table 3. The total ion current diagrams of the saturated hydrocarbons predominantly displayed slight bimodal distribution pattern (Fig. 3a–c). Values of C_{21}/C_{22+} and $(C_{21}+C_{22})/(C_{28}+C_{29})$ ratios are in the range of 0.36–1.58 with an average of 0.66 and the range of 0.67–2.19 with an average of 1.16, respectively, which indicate their related source rocks have predominantly aquatic organism inputs and subordinate terrestrial organic matter input (Curiale and Bromley, 1996). Moreover, the CPI and

OEP ratios vary from 0.93 to 1.12 and 0.84 to 1.10, respectively, which may indicate mature oils (Bray and Evans, 1961; Scalan and Smith, 1970) or predominant contribution of bacteria and algae (Peters et al., 2005).

4.4. Steranes

The relative abundances of regular steranes are commonly used to reflect oil origins and used for oil-source correlation analysis. Particularly, the relative abundance of C₂₇ regular steranes reflect the lower aquatic organisms or red algae contributions (Volkman et al., 1986), and C₂₉ regular steranes reveal the terrestrial higher plants or green algae contributions (Sepúlveda et al., 2009; Brocks et al., 2017). Oil samples No.1-29 show similar V-shaped distribution pattern of C₂₇–C₂₉ steranes (Fig. 4a and b), which suggesting that they have a similar organic matter composition that dominated by algal organic matter. Whereas samples No. 30–32 have the lowest C₂₇/C₂₉ $\alpha\alpha\alpha$ R sterane ratio (0.26–0.38), indicating a different source rock with high contribution of terrigenous organic matter (Volkman et al., 1986) or planktonic green algae (Brocks et al., 2017). Diasteranes can be formed by the catalysis of clay minerals under oxidizing conditions, hence are widely used to reflect the depositional condition (Rubinstein et al., 1975; Li et al., 2003). The relatively higher ratio of C₂₇ diasteranes to C₂₇ regular steranes (C₂₇Dia/C₂₇St) of samples No. 1–25 than other oils

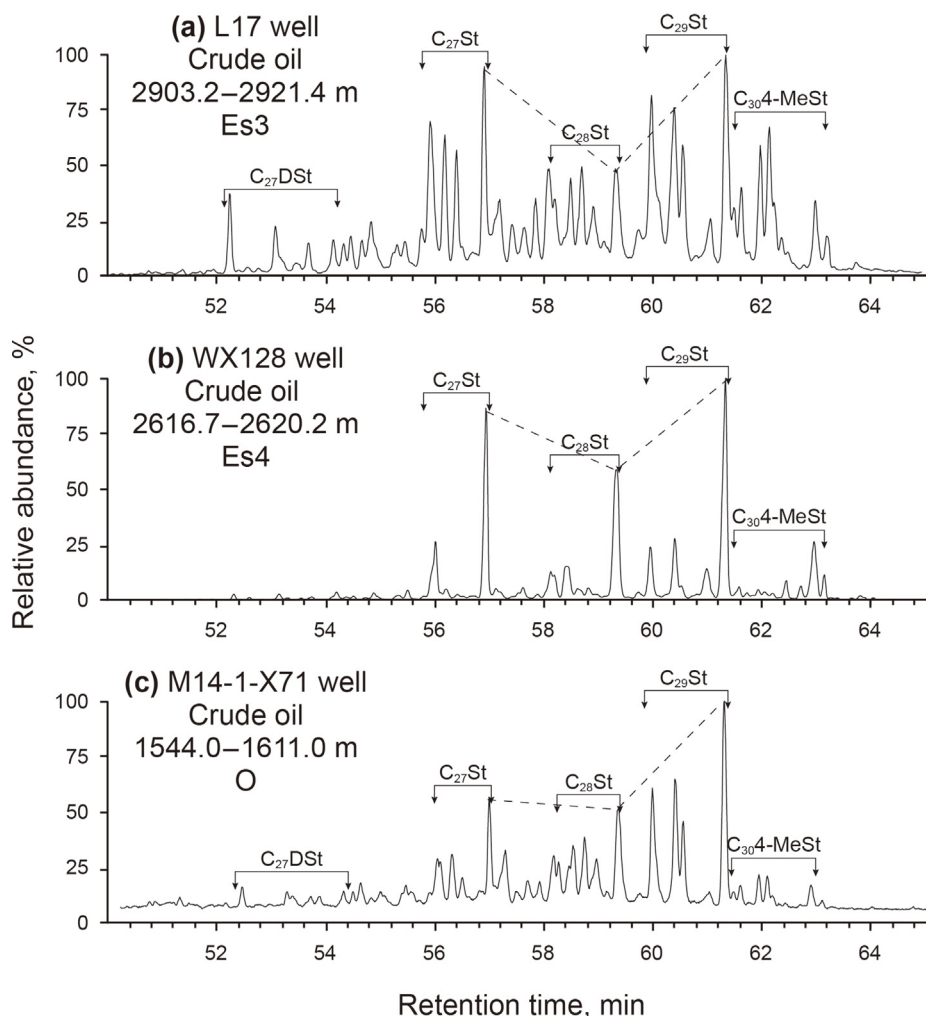


Fig. 4. Partial *m/z* 217 mass chromatograms showing the distribution of sterane series in crude oils from the Dongying Depression.

suggesting slightly anoxic depositional conditions, which is consistent with the depositional condition of the Es³_L source rocks (Zhang et al., 2009). Though samples No. 30–32 also have high C₂₇Dia/C₂₇St ratio, these oils were not derived from the Es³_L source rocks, due to their abnormally higher concentration of C₂₉ steranes than samples No. 1–25 (Fig. 4).

The C₃₀ 4 α -methylsteranes are prominent components of sterols from lacustrine environments (Brassell et al., 1986; Summons et al., 1992). In the Bohai Bay Basin, abundant C₃₀ 4 α -methylsteranes were identified in the Es³_L source rock, which were contributed by the enriched dinoflagellate algae (i.e., *Bohaidina* and *Paraboahaidina*) in the Es³_L source rock (Chen et al., 1996; Hao et al., 2009b). So that 4 α -methylsteranes/C₂₉ steranes ratio (4-Me/C₂₉St) can be used for oil-source and oil-oil correlations in the study area. The relatively higher values of 4-Me/C₂₉St of samples No. 1–25 (Fig. 4a) indicating that there is a significant contribution of the Es³_L source rock to these oils. In addition, among all the oils, samples No. 26–29 have the lowest isomerization degree of steranes and reflect their lower maturity than other oils, this was discussed in detail in the thermal maturity section. Overall, oils can be preliminarily classified into three types by the distribution characteristics of steranes, with oil samples No. 1–25, No. 26–29 and No. 30–32 each being one type oil.

4.5. Tricyclic terpanes and hopanes

Tricyclic terpanes and tetracyclic terpanes (TT and TeT) are widely used to determine the biogenetic sources of oils and source rocks. C₁₉TT, C₂₀TT and C₂₄TeT usually indicate terrigenous organic matter inputs while C₂₃TT is more abundant in marine oils or saline lacustrine oils (Philp and Gilbert, 1986; Zhang and Huang, 2005; Xiao et al., 2019b, 2019d). Samples No. 30–32 were dominated by C₂₁TT within the C₁₉–C₂₃ tricyclic terpanes (Fig. 5c) and have relatively higher concentration of tricyclic terpanes than samples No. 1–29, which may be taken as evidence for a contribution from the algae *Tasmanite* in the fresh lacustrine (De Grande et al., 1993; Pang et al., 2003; Xiao et al., 2019b). Moreover, these three oils have much lower values of C₁₉/C₂₃TT (0.13–0.14) and C₂₄TeT/C₂₆TT (0.25–0.36) than those of all the other oils (C₁₉/C₂₃TT, 0.10–0.88; C₂₄TeT/C₂₆TT, 0.44–1.13) (Table 4), denoting limited terrigenous organic matters contributed to their related source rocks. Although samples No. 1–29 show similar distribution pattern of C₁₉–C₂₃ tricyclic terpanes with C₂₃TT as the dominant homologue (Fig. 5a and b), samples No. 26–29 have relative lower values of C₁₉/C₂₃TT (0.10–0.19) and C₂₄TeT/C₂₆TT (0.49–0.67) than that of samples No. 1–25 (Table 4). This biomarker assemblage means that the related source rock of samples No. 26–29 contains abundant contribution

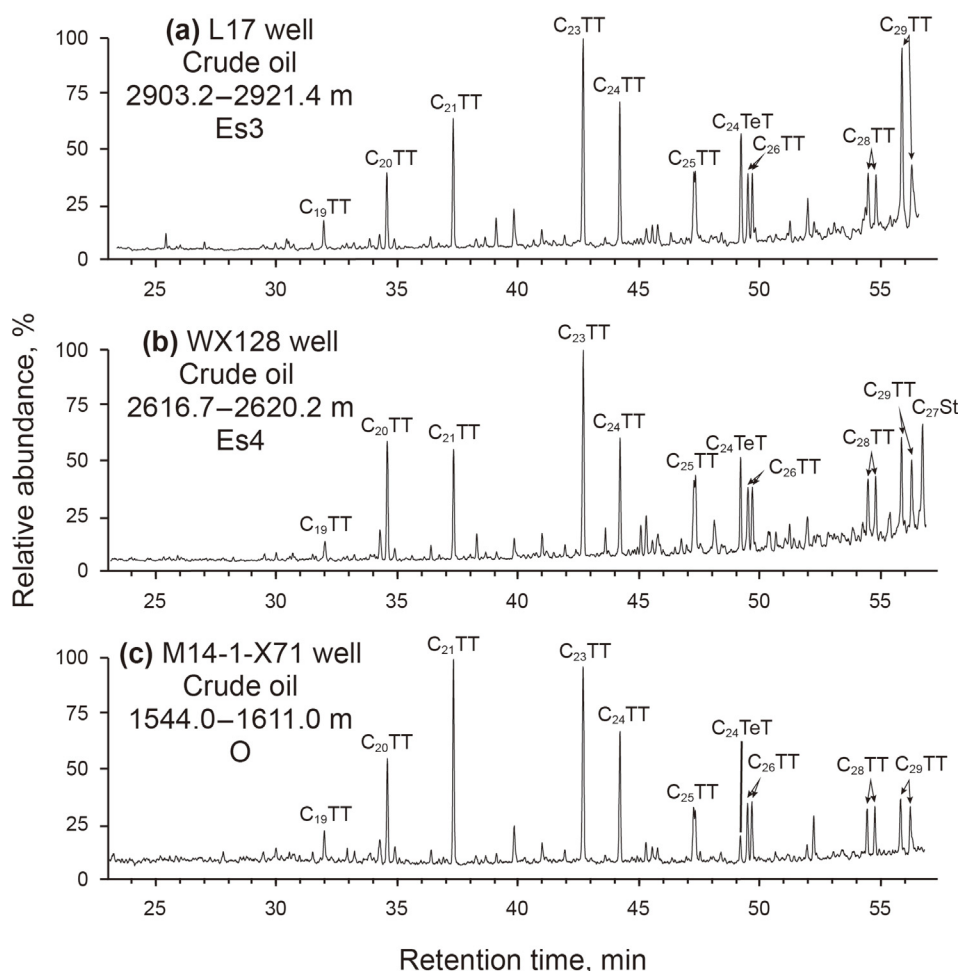


Fig. 5. Partial m/z 191 mass chromatograms showing the distribution of tricyclic terpanes in crude oils from the Dongying Depression.

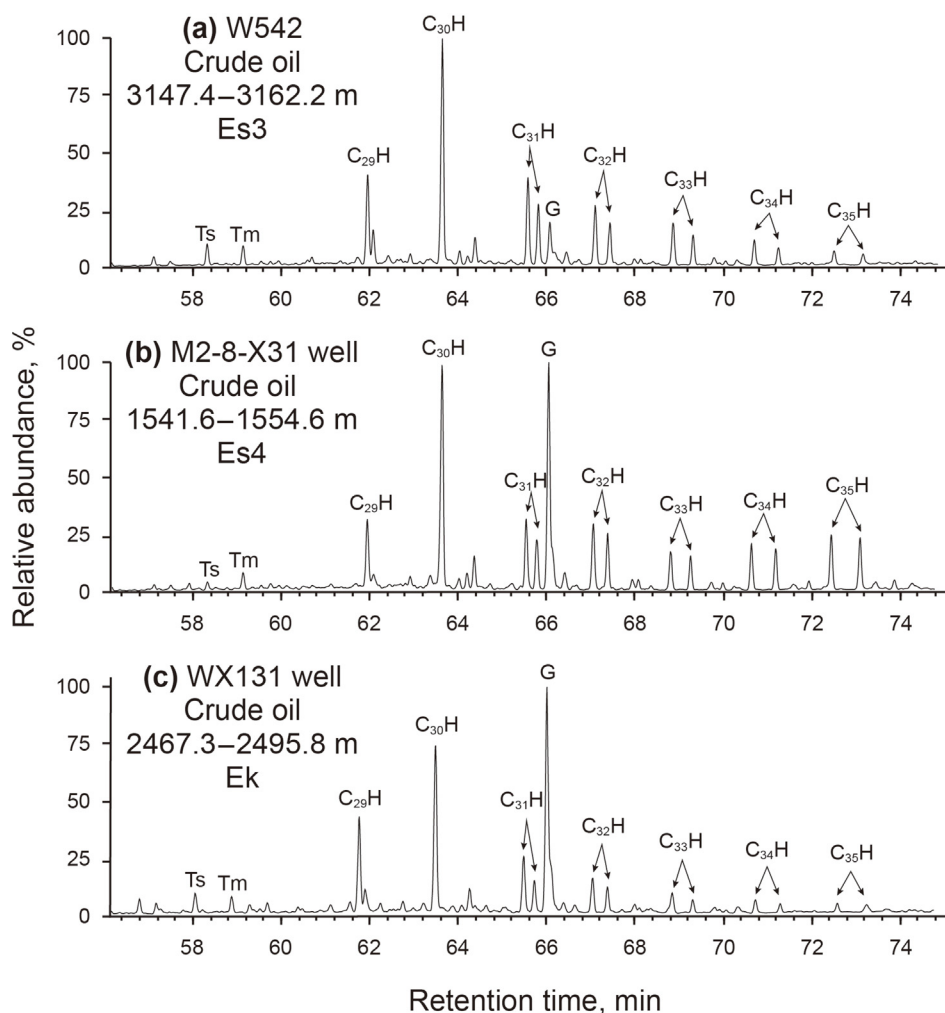


Fig. 6. Partial m/z 191 mass chromatograms showing the distribution of hopane series in crude oils from the Dongying Depression.

of algal organic matter and minor terrigenous organic matter, which is accordant with the Es4^U source rock (Zhang et al., 2003, 2009; Zhu and Jin, 2003; Zhu et al., 2004a).

Interestingly, oil samples No. 1–25 have different amounts of the two peaks of C₂₉TT diastereomeric pair (Fig. 5a) and the peak height of C₂₉TT even exceed C₂₃TT, which may be influenced by C₂₇ sterane isomers because of the higher sterane isomerization degree. Because of the low isomerization degree of steranes in samples No. 26–29, C₂₉TT were unaffected by C₂₇ sterane isomers, but the peak of C₂₇ $\alpha\alpha\alpha$ R sterane were still identified behind the C₂₉TT diastereomeric pair (Fig. 5b). Whereas this scenario almost disappeared in samples No. 30–32, owing to the lowest concentration of C₂₇ steranes (Fig. 5c). In short, three oil types can also be classified based on the characteristics of C₁₉–C₂₉TT and C₂₄TeT.

C₃₀–C₃₅ homohopanes are determined to be originated from bacteriohopanetetrol, and C₃₅/C₃₄ 22S hopanes ratio (C₃₅/C₃₄ 22S H) are effective parameters to infer redox conditions (Peters et al., 2005). Gammacerane is believed to form in a stratified water column (Sinninghe Damsté et al., 1995; Sepúlveda et al., 2009) that can be caused by both hypersalinity and temperature gradient. Thus, abundant gammacerane and high C₃₅/C₃₄ 22S H ratio are usually occur in source rocks that deposited in the high salinity environment (Fu et al., 1986; Chen et al., 1996; Zhang et al., 2003).

The relative abundances of C₃₀–C₃₅ homohopanes and gammacerane significantly varies in our samples (Fig. 6). According to

distribution patterns of hopane series, as shown in Fig. 5, crude oils can also be classified into three types. Samples No. 1–25 have low abundance of gammaceranes and relatively low C₃₅/C₃₄ 22S H ratio (Fig. 6a and Table 4), indicating a fresh to brackish water lacustrine environment of the related source rock which well consists with the Es3^L source rock (Pang et al., 2003; Zhang et al., 2003, 2009; Li et al., 2010). Samples No. 26–32 have abundant gammaceranes with significant higher values of G/C₃₀ hopane (0.48–1.91) than samples No. 1–25 (0.05–0.44) (Fig. 6b and Table 4), suggesting stratified water or sulfate-reducing or saline depositional conditions. Moreover, samples No. 26–29 contain obviously high abundances of C₃₅ hopanes (Fig. 6b) with the C₃₅/C₃₄ 22S H ratio in the range of 1.15–1.30 (Table 4). This scenario indicates that these four oils probably have different source rocks with other oils, but possibly derived from the Es4^U source rock that formed in strongly reductive and saline to brackish depositional condition (Li et al., 2003; Pang et al., 2003; Zhu and Jin, 2003; Zhang et al., 2009). Although samples No. 30–32 also have abundant gammacerane, dominance of C₃₅ and/or C₃₄ hopanes did not appear at the same time (Fig. 6c). In addition, the cross plots of G/C₃₀H versus Pr/Ph, C₃₅/C₃₄ 22S H, C₂₉St/C₃₀H and 4-Me/C₂₉St show that three oil types can be distinguished clearly (Fig. 7), and type I, II, and III oils include the samples 1–25, 26–29, and 30–32, respectively.

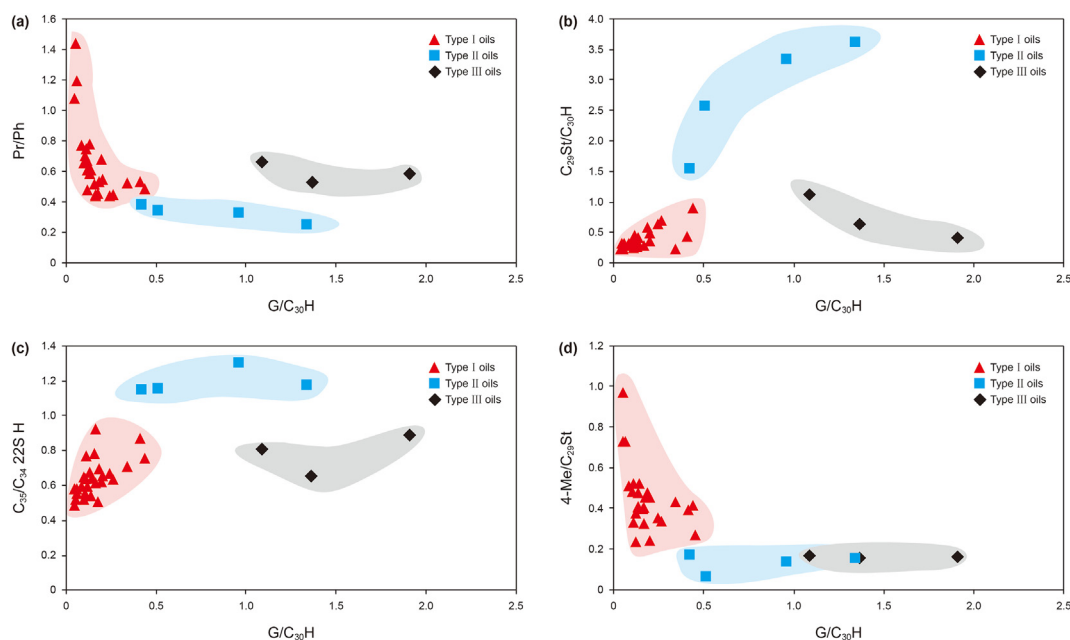


Fig. 7. Cross plots of G/C₃₀H vs. Pr/Ph (a), G/C₃₀H vs. C₂₇St/C₃₀H (b), G/C₃₀H vs. C₃₅/C₃₄ 22 S H (c) and 4-Me/C₂₉St (d) showing the differences between three oil types.

4.6. Hierarchical cluster analysis

Hierarchical cluster analysis (HCA) is an effective way to distinguish crude oils (Peters et al., 2007; Hao et al., 2009a, 2009b; Xiao et al., 2019a), and was applied in crude oil classification in this study. Statistical Package for the Social Sciences (SPSS Inc.) was used for HCA, and the Euclidean measure interval and between-groups linkage method were used in HCA. Eleven parameters were selected (parameters R1-R11 in Table 4), which are related to

depositional environments and/or organic matter input, and almost not affected by thermal maturation or biodegradation. The HCA method clearly classify the oils samples into three types (Fig. 8), and type I, II, and III oils include the samples 1–25, 26–29, and 30–32, respectively.

Type I oils (Sm. No. 1–25) have relative highest values of Pr/Ph, C₂₇Dia/C₂₇St, 4-Me/C₂₉St, C₁₉/C₂₃TT and C₂₄TeT/C₂₆TT ratios, and lowest values of C₂₉St/C₃₀H, G/C₃₀H and C₃₅/C₃₄22S H ratios (Table 4). The biomarker assemblage of type I oils suggests their related source rocks were deposited in freshwater and suboxic environments with algal and terrigenous organic matters input, which correlates well with the Es₃^L source rock (Zhang et al., 2003; Li et al., 2010). Thus, type I oils are interpreted to originate from or mostly from the Es₃^L source rock.

Type II oils (Sm. No. 26–29) display high C₂₉St/C₃₀H, G/C₃₀H and C₃₅/C₃₄22S H ratios and low Pr/Ph, C₂₇Dia/C₂₇St, 4-Me/C₂₉St, C₁₉/C₂₃TT and C₂₄TeT/C₂₆TT ratios. The low C₁₉/C₂₃TT, and C₂₄TeT/C₂₆TT ratios (Table 4), which are completely different from the Es₃^L source rock. The biomarker assemblage of type II oils reveals their related source rocks were deposited in a strongly anoxic, reducing and saline lake environments with dominant algal organic matter

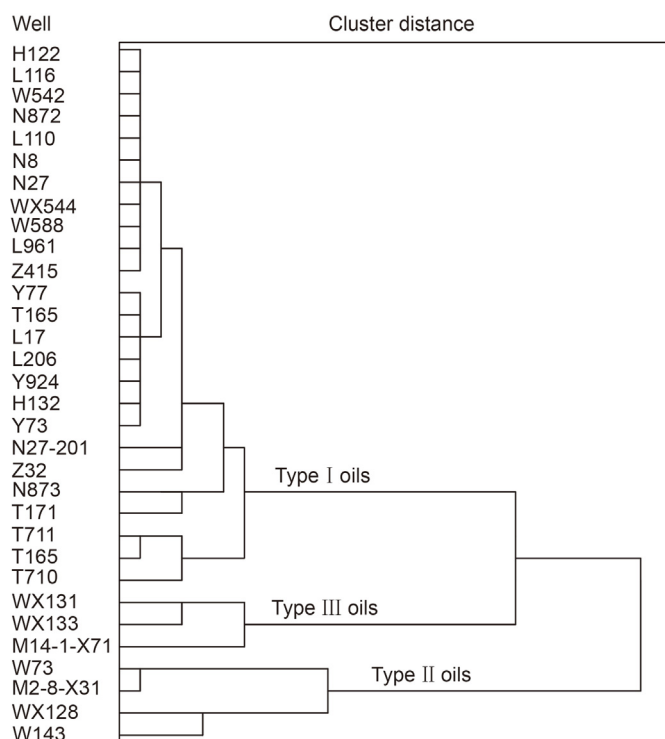


Fig. 8. Hierarchical cluster analysis showing the crude oil types.

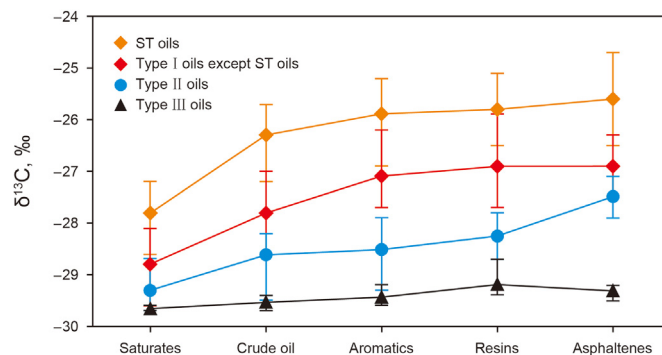


Fig. 9. Carbon isotope distribution patterns of crude oils showing the average values and ranges of δ¹³C for each fraction of three oil types in the Dongying Depression, ST oils = oils from the ST oilfield.

input, which is consistent with the Es^{4L} source rock (Zhu et al., 2004a; Zhang et al., 2009). Therefore, the type II oils were interpreted to be mainly derived from the Es^{4L} source rock.

Type III oils (Sm. No. 30–32) are rich in C₂₉ steranes, tricyclic terpanes and gammacerane, and are markedly different from type I and II oils (Table 4). 4-Me/C₂₉St, C₂₉St/C₃₀H, and Pr/Ph ratios of type III oils are relatively low (Table 4). Based on the biomarker characteristics of these oils, it can be inferred that the related source rocks were potentially deposited in a slightly reducing, perhaps saline and stratified, water environment, which is distinctly different from the Es^{3L} source rock but seems to be similar to the Es^{4U} source rocks. However, the related source rocks of type III oils have greater bacteria/algae inputs that could produce large quantities of C₂₉ steranes and tricyclic terpanes, which revers its relationship with the Es^{4U} source rocks. Based on the above, the type III oils are considered to have no obvious oil source relationship with the known source rocks including the Es^{3L} and the Es^{4U} source rocks.

4.7. Stable carbon isotope compositions

The stable carbon isotope composition is also a main approach on oil-oil and oil-source correlations (Peters et al., 1986; Galimov, 2006). Crude oils and their fractions in the Dongying Depression have wide range of δ¹³C values (Fig. 9), indicating that crude oils have different sources. Type I oils have more heavier δ¹³C values than type II and III oils (Fig. 9), indicating that the source rock of type I oils contains more contribution of terrigenous organic matter than type II and III oils. Type III oils have the lowest δ¹³C values (<−30‰) suggesting that related source rock was dominated by algae and aquatic organisms (Galimov, 2006), this further implies that the higher concentration of C₂₉ steranes of type III oils were sourced from some planktonic algae or bacteria rather than terrigenous higher plants (Kodner et al., 2008; Summons and Erwin, 2018).

Generally, according to the biomarker compositions and sulfur content, oils from the ST oilfield with low sulfur content were proposed to be originated from the Es^{3L} source rock (Zhu et al.,

2004b). Notably, the oils from the ST oilfield were also confirmed to belong to type I oils derived from the Es^{3L} source rocks based on biomarker compositions (Tables 3 and 4) and low sulfur content (0.07–0.21). However, they contain the extremely high values of δ¹³C, which is completely different from other type I oils. The distinction of δ¹³C values with type I oils possibly reflects that the related source rocks have slightly different contributions. Enrichment of ¹³C in the oils from the ST oilfield is indicative of relative more contributions from terrigenous land plants or benthic macro algae (Galimov, 2006), which is consistent with the high values of C₁₉/C₂₃TT and C₂₄TeT/C₂₆TT ratios (Table 4). The ST oilfield is located in the Northern Steep Slope of the Dongying Depression, in which widely developed alluvial fans with more terrigenous organic matter inputs during the deposition period of the Shahejie Formation (Ping et al., 2017).

4.8. Distribution of crude oils

Based on the analysis of biomarker compositions and stable carbon isotope compositions, these investigated oils were classified into three types. Furthermore, the spacial distribution characteristics of these three oil types were analyzed.

From the northwest to the southeast (from ZJ oilfield through ST oilfield, XH oilfield, LJL oilfield, NZ oilfield and WJG oilfield to BMH oilfield), systematic variations in biomarker compositions occur: (1) 4-Me/C₂₉St and C₂₄TeT/C₂₆TT ratios keep high in northwestern oilfields for type I oils but decrease in WJG and BMH oilfields for type II and III oils (Fig. 10a and b); (2) C₁₉/C₂₃TT ratio reach the highest in ST oilfield and decrease from XH to BMH oilfields (Fig. 10c); (3) G/C₃₀H ratio keep low from ZJ to WJG oilfield for type I oils but increase in WJG and BMH oilfields for type II and III oils (Fig. 10d); (4) C₂₇Dia/C₂₇St ratio decrease from ZJ to BMH oilfields (Fig. 10e); (5) Pr/Ph ratios are high for type I oils from ZJ to WJG oilfield but relative low for type II and III oils in WJG and BMH oilfields (Fig. 10f). These clear trends display the various biological origins and depositional environments of the related source rocks, also imply the different distribution pattern of three oil types.

According to well location of different type oils, it can be seen

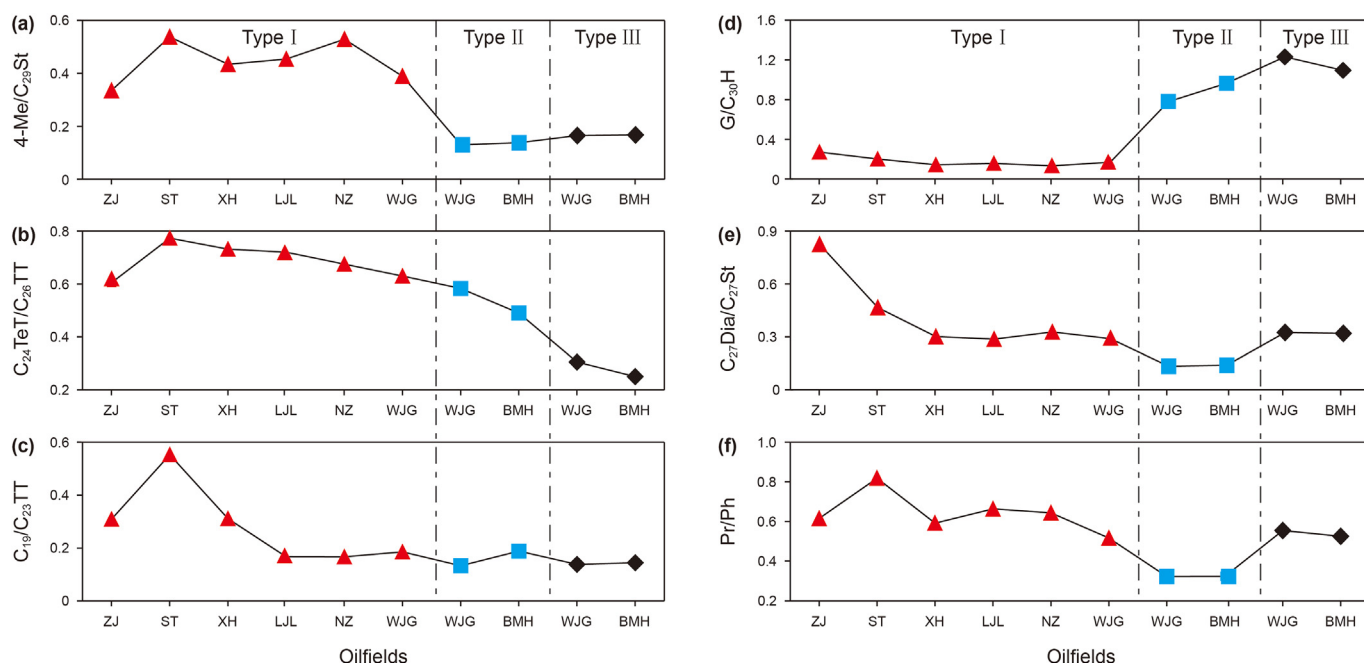


Fig. 10. The average values of various parameters for oils from each oilfield.

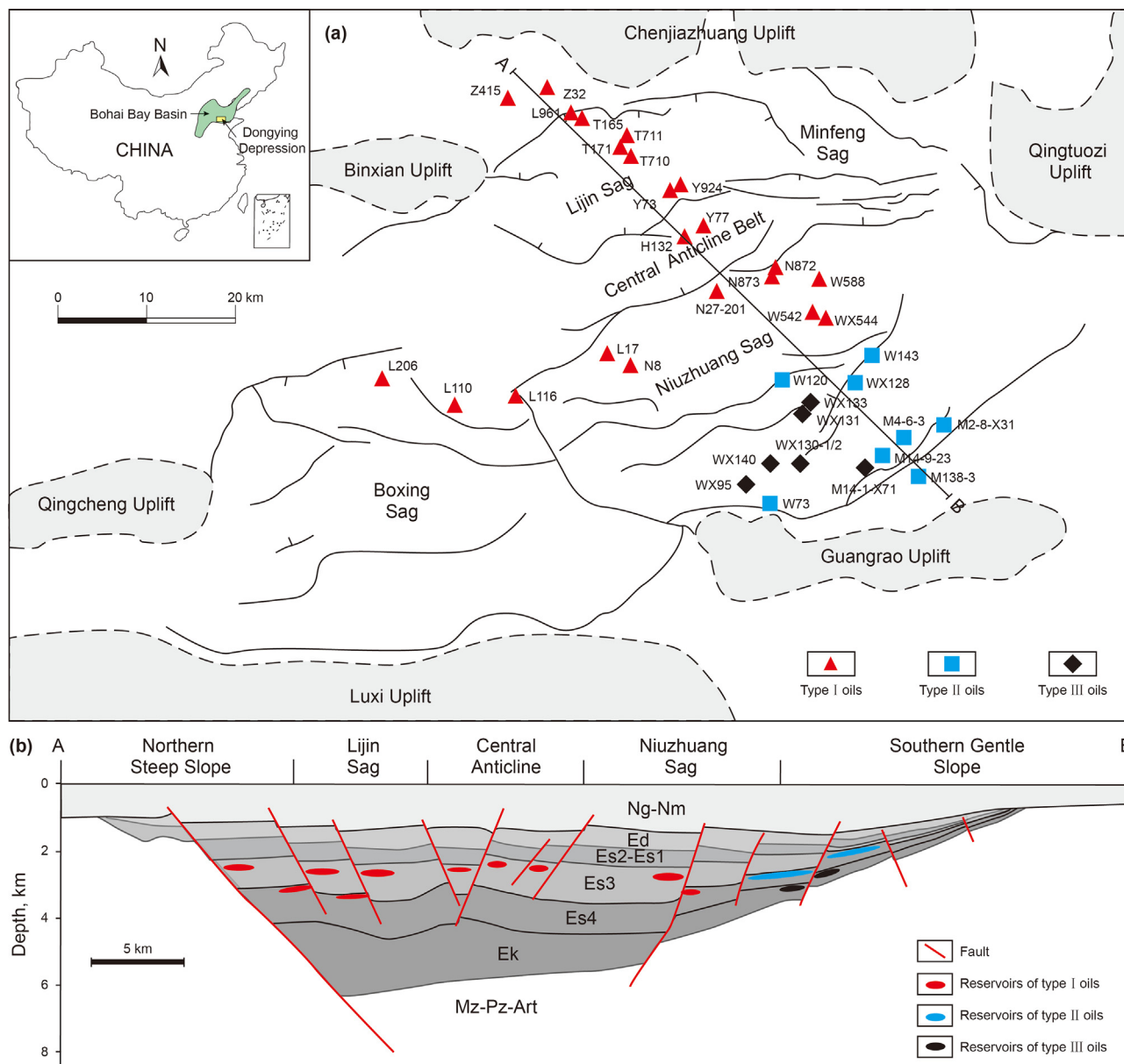


Fig. 11. Spatial distribution patterns of crude oils in the Dongying Depression.

that type I oils were extensively distributed in the Niuzhuang Sag, Central Anticline, Lijin Sag and Northern Steep Slope, which are mainly contributed from the Es3^L source rock. Type II and III oils were restrictedly distributed in the Southern Gentle Slope, and considered to be from the Es4^U source rock and unclear source rock, respectively (Fig. 11a). In addition, type I oils were distributed in both Es3 and Es4 reservoirs, and type II oils were mainly discovered in the Es4 reservoirs, whereas type III oils mainly occur in the Ek and Ordovician buried hill reservoirs (Fig. 11b), consistent with previous findings (Li et al., 2005; Zhan et al., 2019).

The Es3^L source rocks were mainly distributed in the center and northern of the depression, and the Es3^L-derived oils were proposed to migrate short distances and then accumulated in traps close to the generative kitchen (Zhu et al., 2004a; Zhang et al., 2012). According to the basic theory that the special distribution of crude oils is significantly controlled by source rock location, this phenomenon explains the distribution of type I oils mainly in the center and northern of the depression. In addition, numerous

basin-dip faults were developed in the northern slope (Li, 2004), providing opportunities for the Es3^L source rocks to be intercepted directly by the Es4 reservoir, which allowed that Es3^L-derived oils were discovered in the Es4 reservoirs. The absence of the Es3^L source rocks in the southern of the depression caused the scarce distribution of type I oils in the Southern Gentle Slope (Fig. 11).

The Es4^U source rocks are covered by the thick mudstone of the Es3 interval, the intense oil generation of these mudstones caused widespread overpressure in the Es3 and Es4 intervals (Guo et al., 2010), which prevented a massive vertical migration of the Es4^U-derived oils. And the Es4^U and Es3^L mudstones can also serve as an effective caprock to prevent the vertical migration. These reasons promoted the large-scale lateral migration of the Es4^U-derived oils along the common horizontal fractures in the mudstones and the laterally distributed sandstone layers within the Es4 interval. This resulted in the Es4^U-derived oils being mainly distributed in the southern of the depression with relatively shallow burial depth and low pressure.

Recently, type III oils were mainly found in the Ek reservoirs and the Ordovician buried hill reservoir in the southern depression, but no discovery in the northern depression. We can reasonably speculate that the shallow depth of Ek (~2500 m in WX131 well) and the Ordovician reservoirs (~1550 m in M14-1-X71 well) in the southern depression makes the type III oils easy to be discovered. Another possibility is that the source rocks of type III oils were mainly deposited in the south. Therefore, we are eagerly expecting that through deep drilling in the study area, more commercial oil accumulations of type III oils and its corresponding source rocks can be discovered in the future.

5. Conclusion

Geochemical investigation of 32 crude oils from the Dongying Depression suggests that crude oils can be discriminated into three oil types. Based on the oil-source correlation analysis, type I oils were determined to be mainly contributed by the Es^{3L}-derived oils and type II oils as typical immature oils were derived from the Es^{4U} source rocks. However, type III oils were not matchable with any discovered source rocks. Type III oils have significantly high abundances of gammacerane, tricyclic terpanes and C₂₉ steranes but the lowest δ¹³C values of all the crude oils, which were not matchable with any discovered source rocks and implies the related source rocks have markedly different biological origins and depositional environments with the Es^{4U} and Es^{3L} source rocks. This scenario indicates a probable undiscovered source rock in the older strata in the Dongying Depression.

Vertically, type I oils occurred in the Es³ and Es⁴ reservoirs, type II oils in the Es⁴ reservoirs, but type III oils were discovered in the Ek and Ordovician reservoirs. Horizontally, type I oils were mainly distributed in the northern slope and center of the depression, whereas type II and III oils were mainly discovered in the southern slope of the depression.

Acknowledgements

This work was funded by National Natural Science Foundation of China (Grants Nos. 41972127 and U19B6003). The authors would like to thank the executive editor and two reviewers for their constructive comments and suggestions which significantly improved the quality of the manuscript.

References

Bennett, B., Fustic, M., Farrimond, P., et al., 2006. 25-Norhopanes: formation during biodegradation of petroleum in the subsurface. *Org. Geochem.* 37, 787–797. <https://doi.org/10.1016/j.orggeochem.2006.03.003>.

Brassell, S., Eglinton, G., Marlowe, I., et al., 1986. Molecular stratigraphy: a new tool for climatic assessment. *Nature* 320, 129–133. <https://doi.org/10.1038/320129a0>.

Bray, E.E., Evans, E.D., 1961. Distribution of n-paraffins as a clue to recognition of source beds. *Geochem. Cosmochim. Acta* 22, 2–15. [https://doi.org/10.1016/0016-7037\(61\)90069-2](https://doi.org/10.1016/0016-7037(61)90069-2).

Brocks, J.J., Jarrett, A.J.M., Sirantoine, et al., 2017. The rise of algae in Cryogenian oceans and the emergence of animals. *Nature* 548, 578–581. <https://doi.org/10.1038/nature23457>.

Chen, J., Bi, Y., Zhang, J., et al., 1996. Oil-source correlation in the Fulin basin, Shengli petroleum province, East China. *Org. Geochem.* 24, 931–940. [https://doi.org/10.1016/S0146-6380\(96\)00049-6](https://doi.org/10.1016/S0146-6380(96)00049-6).

Curiale, J.A., Bromley, B.W., 1996. Migration induced compositional changes in oils and condensates of a single field. *Org. Geochem.* 24, 1097–1113. [https://doi.org/10.1016/S0146-6380\(96\)00099-X](https://doi.org/10.1016/S0146-6380(96)00099-X).

De Grande, S.M.B., Aquino Neto, F.R., Mello, M.R., 1993. Extended tricyclic terpanes in sediments and petroleum. *Org. Geochem.* 20, 1039–1047. [https://doi.org/10.1016/0146-6380\(93\)90112-0](https://doi.org/10.1016/0146-6380(93)90112-0).

Fu, J., Sheng, G., Peng, P., et al., 1986. Peculiarities of salt lake sediments as potential source rocks in China. *Org. Geochem.* 10, 119–126. [https://doi.org/10.1016/0146-6380\(86\)90015-X](https://doi.org/10.1016/0146-6380(86)90015-X).

Galimov, E.M., 2006. Isotope organic geochemistry. *Org. Geochem.* 37, 1200–1262. <https://doi.org/10.1016/j.orggeochem.2006.04.009>.

Guo, X., He, S., Liu, K., et al., 2010. Oil generation as the dominant overpressure mechanism in the cenozoic dongying depression, Bohai Bay Basin, China. *AAPG Bull* 94, 1859–1881. <https://doi.org/10.1306/05191009179>.

Hao, F., Zhou, X., Zhu, Y., et al., 2009a. Mechanisms for oil depletion and enrichment on the shijituo uplift, Bohai Bay Basin, China. *AAPG Bull* 93, 1015–1037. <https://doi.org/10.1306/04140908156>.

Hao, F., Zhou, X., Zhu, Y., et al., 2009b. Mechanisms of petroleum accumulation in the Bozhong sub-basin, Bohai Bay Basin, China. Part 1: origin and occurrence of crude oils. *Mar. Petrol. Geol.* 26, 1528–1542. <https://doi.org/10.1016/j.marpetgeo.2008.09.005>.

Huang, H., Pearson, M.J., 1999. Source rock palaeoenvironments and controls on the distribution of dibenzothiophenes in lacustrine crude oils, Bohai Bay Basin, eastern China. *Org. Geochem.* 30, 1455–1470. [https://doi.org/10.1016/S0146-6380\(99\)00126-6](https://doi.org/10.1016/S0146-6380(99)00126-6).

Kodner, R.B., Pearson, A., Summons, R.E., et al., 2008. Sterols in red and green algae: quantification, phylogeny, and relevance for the interpretation of geologic steranes. *Geobiology* 6, 411–420. <https://doi.org/10.1111/j.1472-4669.2008.00167.x>.

Li, P., 2004. Oil/gas distribution patterns in dongying depression, Bohai Bay Basin. *J. Petrol. Sci. Eng.* 41, 57–66. [https://doi.org/10.1016/S0920-4105\(03\)00143-8](https://doi.org/10.1016/S0920-4105(03)00143-8).

Li, S., Pang, X., Li, M., et al., 2003. Geochemistry of petroleum systems in the Niuzhuang south slope of Bohai Bay Basin—part 1: source rock characterization. *Org. Geochem.* 34, 389–412. [https://doi.org/10.1016/S0146-6380\(02\)00210-3](https://doi.org/10.1016/S0146-6380(02)00210-3).

Li, S., Pang, X., Li, M., et al., 2005. Geochemistry of petroleum systems in the Niuzhuang South Slope of Bohai Bay Basin: Part 4. Evidence for new exploration horizons in a maturely explored petroleum province. *Org. Geochem.* 36, 1135–1150. <https://doi.org/10.1016/j.orggeochem.2005.03.004>.

Li, S., Pang, X., Jin, Z., et al., 2010. Molecular and isotopic evidence for mixed-source oils in subtle petroleum traps of the Dongying South Slope, Bohai Bay Basin. *Mar. Petrol. Geol.* 27, 1411–1423. <https://doi.org/10.1016/j.marpetgeo.2010.04.004>.

Liu, H., Jiang, Y., Zhang, L., et al., 2009. Characteristics of petroleum system and oil—source in Dongying Depression. *Geol. J. China Univ.* 15, 93–99 (in Chinese). [https://doi.org/10.1016/S1003-6326\(09\)60084-4](https://doi.org/10.1016/S1003-6326(09)60084-4).

Meng, J., Liu, L., Jiang, Z., et al., 2011. Geochemical characteristics of crude oil and oil-source correlation of the Paleogene red bed in the South slope of the dongying depression, Bohai Bay Basin, China. *Energ. Explor. Exploit.* 29, 397–412. <https://doi.org/10.1260/0144-5987.29.4.397>.

Niu, Z., Meng, W., Wang, Y., et al., 2021. Characteristics of trace elements in crude oil in the east section of the south slope of Dongying Sag and their application in crude oil classification. *J. Petrol. Sci. Eng.* 209, 109833. <https://doi.org/10.1016/j.petrol.2021.109833>.

Pang, X., Li, M., Li, S., et al., 2003. Geochemistry of petroleum systems in the Niuzhuang South Slope of Bohai Bay Basin. Part 2: evidence for significant contribution of mature source rocks to “immature oils” in the Bamihan field. *Org. Geochem.* 34, 931–950. [https://doi.org/10.1016/S0146-6380\(03\)00032-9](https://doi.org/10.1016/S0146-6380(03)00032-9).

Peters, K.E., Moldowan, J.M., Schoell, M., et al., 1986. Petroleum isotopic and biomarker composition related to source rock organic matter and depositional environment. *Org. Geochem.* 10, 17–27. [https://doi.org/10.1016/0146-6380\(86\)90006-9](https://doi.org/10.1016/0146-6380(86)90006-9).

Peters, K.E., Walters, C.C., Moldowan, J.M., 2005. *The Biomarker Guide, second ed.* Cambridge University Press, New York, pp. 538–575.

Peters, K.E., Ramos, L.S., Zumbege, J.E., et al., 2007. Circum-Arctic petroleum systems identified using decision-tree chemometrics. *AAPG Bulletin* 91, 877–913. <https://doi.org/10.1306/12290606097>.

Philp, R.P., Gilbert, T.D., 1986. Biomarker distributions in Australian oils predominantly derived from terrigenous source material. *Org. Geochem.* 10, 73–84. [https://doi.org/10.1016/0146-6380\(86\)90010-0](https://doi.org/10.1016/0146-6380(86)90010-0).

Ping, H., Chen, H., Jia, G., 2017. Petroleum accumulation in the deeply buried reservoirs in the northern Dongying Depression, Bohai Bay Basin, China: new insights from fluid inclusions, natural gas geochemistry, and 1-D basin modeling. *Mar. Petrol. Geol.* 80, 70–93. <https://doi.org/10.1016/j.marpetgeo.2016.11.023>.

Rubinstein, I., Sieskind, O., Albrecht, P., 1975. Rearranged sterenes in a shale: occurrence and simulated formation. *Journal of the Chemical Society, Perkin Transactions 1*, 1833–1836. <https://doi.org/10.1039/p19750001833>.

Scalan, E.S., Smith, J.E., 1970. An improved measure of the odd-even predominance in the normal alkanes of sediment extracts and petroleum. *Geochem. Cosmochim. Acta* 34, 611–620. [https://doi.org/10.1016/0016-7037\(70\)90019-0](https://doi.org/10.1016/0016-7037(70)90019-0).

Sepúlveda, J., Wendler, J., Leider, A., et al., 2009. Molecular isotopic evidence of environmental and ecological changes across the Cenomanian-Turonian boundary in the Levant Platform of central Jordan. *Org. Geochem.* 40, 553–568. <https://doi.org/10.1016/j.orggeochem.2009.02.009>.

Sinninghe Damst'e, J.S., Kenig, F., Koopmans, M.P., et al., 1995. Evidence for gammacerane as an indicator of water column stratification. *Geochem. Cosmochim. Acta* 59, 1895–1900. [https://doi.org/10.1016/0016-7037\(95\)00073-9](https://doi.org/10.1016/0016-7037(95)00073-9).

Summons, R.E., Erwin, D.H., 2018. Chemical clues to the earliest animal fossils. *Science* 361, 1198–1199. <https://doi.org/10.1126/science.aau9710>.

Summons, R.E., Thomas, T., Maxwell, J.R., et al., 1992. Secular and environmental constraints on the occurrence of dinosterane in sediments. *Geochem. Cosmochim. Acta* 56, 2437–2444. [https://doi.org/10.1016/0016-7037\(92\)90200-3](https://doi.org/10.1016/0016-7037(92)90200-3).

Volkman, J.K., Alexander, R., Kagi, R.L., et al., 1983. Demethylated hopanes in crude oils and their applications in petroleum geochemistry. *Geochem. Cosmochim. Acta* 47, 785–794. [https://doi.org/10.1016/0016-7037\(83\)90112-6](https://doi.org/10.1016/0016-7037(83)90112-6).

Volkman, J.K., Allen, D.I., Stevenson, P.L., et al., 1986. Bacterial and algal hydrocarbons in sediments from a saline Antarctic lake, Ace Lake. *Org. Geochem.* 10,

- 671–681. [https://doi.org/10.1016/S0146-6380\(86\)80003-1](https://doi.org/10.1016/S0146-6380(86)80003-1).
- Wang, Q., Huang, H., Li, Z., 2021. Mixing scenario of a variegated oil in the Dongying depression, Bohai Bay Basin. *Fuel* 294, 120589. <https://doi.org/10.1016/j.fuel.2021.120589>.
- Xiao, H., Li, M., Liu, J., et al., 2019a. Oil-oil and oil-source rock correlations in the Muglad Basin, Sudan and South Sudan: new insights from molecular markers analyses. *Mar. Petrol. Geol.* 103 (69), 351–365. <https://doi.org/10.1016/j.marpetgeo.2019.03.004>.
- Xiao, H., Li, M., Yang, Z., et al., 2019b. The distribution patterns and geochemical implication of C₁₉–C₂₃ tricyclic terpanes in source rocks and crude oils occurred in various depositional environment. *Geochimica* 48, 161–170. <https://doi.org/10.19700/j.0379-1726.2019.02.006> (in Chinese).
- Xiao, H., Li, M., Wang, T., et al., 2019c. Identification, distribution and geochemical significance of four rearranged hopane series in crude oil. *Org. Geochem.* 128, 103929. <https://doi.org/10.1016/j.orggeochem.2019.103929>.
- Xiao, H., Wang, T., Li, M., et al., 2019d. Geochemical characteristics of Cretaceous Yogou Formation source rocks and oil-source correlation within a sequence stratigraphic framework in the Termit Basin, Niger. *J. Petrol. Sci. Eng.* 172, 360–372. <https://doi.org/10.1016/j.petrol.2018.09.082>.
- Xiao, H., Li, M., Wang, T., et al., 2021a. Four series of rearranged hopanes in the Mesoproterozoic sediments. *Chem. Geol.* 573, 120210. <https://doi.org/10.1016/j.chemgeo.2021.120210>.
- Xiao, H., Wang, T., Li, M., et al., 2021b. Organic geochemical heterogeneity of the Cretaceous Abu Gabra Formation and reassessment of oil sources in the Sufyan sub-basin, Sudan. *Org. Geochem.* 162, 104301. <https://doi.org/10.1016/j.orggeochem.2021.104301>.
- You, B., Ni, Z., Zeng, J., et al., 2020. Oil-charging history constrained by biomarkers of petroleum inclusions in the Dongying Depression, China. *Mar. Petrol. Geol.* 122, 104657. <https://doi.org/10.1016/j.marpetgeo.2020.104657>.
- You, B., Ni, Z., Chen, J., et al., 2021. A distinct oil group in the Dongying Depression, Bohai Bay Basin, China: new insights from norcholestone and triaromatic steroid analyses. *Org. Geochem.* 104316. <https://doi.org/10.1016/j.orggeochem.2021.104316>.
- Zhan, Z., Lin, X., Zou, Y., et al., 2019. Chemometric differentiation of crude oil families in the southern Dongying depression, Bohai Bay Basin, China. *Organic Geochemistry* 127, 37–49. <https://doi.org/10.1016/j.orggeochem.2018.11.004>.
- Zhang, S., Huang, H., 2005. Geochemistry of Palaeozoic marine petroleum from the Tarim Basin, NW China: Part 1. Oil family classification. *Org. Geochem.* 36, 204–214. <https://doi.org/10.1016/j.orggeochem.2005.01.013>.
- Zhang, L., Jiang, Y., Liu, H., et al., 2003. Relationship between source rock and oil accumulation in Dongying Sag. *Petrol. Explor. Develop.* 30, 61–64. <https://doi.org/10.1007/BF02974893> (in Chinese).
- Zhang, L., Liu, Q., Zhu, R., et al., 2009. Source rocks in Mesozoic–Cenozoic continental rift basins, east China: a case from Dongying depression, Bohai Bay Basin. *Org. Geochem.* 40, 229–242. <https://doi.org/10.1016/j.orggeochem.2008.10.013>.
- Zhang, S., Zhang, L., Bao, Y., et al., 2012. Formation fluid characteristics and hydrocarbon accumulation in the Dongying sag, Shengli Oilfield. *Petrol. Explor. Dev.* 39, 423–435. [https://doi.org/10.1016/S1876-3804\(12\)60059-7](https://doi.org/10.1016/S1876-3804(12)60059-7).
- Zhu, G., Jin, Q., 2003. Geochemical characteristics of two sets of excellent source rocks in Dongying Depression. *Acta Sedimentol. Sin.* 21, 506–512. <https://doi.org/10.1007/BF02873154> (in Chinese).
- Zhu, G., Jin, Q., Zhang, S., et al., 2004a. Combination characteristics of lake facies source rock in the Shahejie Formation, Dongying Depression. *Acta Geol. Sin.* 78, 416–427. <https://doi.org/10.12940/jfb.2014.18.4.28> (in Chinese).
- Zhu, G., Jin, Q., Zhou, J., et al., 2004b. Physical properties and genesis of oil in Shengtuo oilfield in Jiyang depression. *Oil Gas Geol.* 25, 9–13. <https://doi.org/10.11743/ogg20040102> (in Chinese).